Journal of Power Sources 196 (2011) 2340–2345

Contents lists available at ScienceDirect

Journal of Power Sources

journal homepage: www.elsevier.com/locate/jpowsour

Zinc morphology in zinc–nickel flow assisted batteries and impact on performance

Yasumasa Ito*, Michael Nyce, Robert Plivelich, Martin Klein, Daniel Steingart, Sanjoy Banerjee

The CUNY Energy Institute, Department of Chemical Engineering, City College of the City University of New York, 140th St at Convent Ave., New York, NY 10031, USA

ARTICLE INFO

Article history:
Received 3 August 2010
Received in revised form 7 September 2010
Accepted 20 September 2010
Available online 30 October 2010

Keywords:
Zinc–nickel oxide battery
Flow battery
Zinc morphology
Coulombic efficiency
Energy efficiency

ABSTRACT

The zinc morphology on repeated charging and discharging in flow-assisted zinc–nickel oxide cells was studied. The results show that higher charge rates cause more dendritic growth of zinc deposition on charging and tend to cause deterioration of battery cells. However, when the electrolyte velocity is higher than 15 cm s^{-1}, the direction of dendrites was distorted toward the flow direction and the internal short circuit was suppressed. Good cycle life was obtained – 1500 cycles at 100% depth of discharge and *C*/2 charge and discharge rate. Also, the battery was scaled up to a 100 Wh prismatic cell, and more than 200 cycles were obtained.

1. Introduction

Economical means of electricity storage will enable efficient use of excess night-time generation capacity to meet demand during peak periods. It also allows more widespread use of baseload low carbon (such as nuclear) and intermittent renewable sources of energy, like the sun, wind and waves. Zinc-based rechargeable batteries such as zinc–nickel oxide are one of the most attractive electrical energy storage systems. The advantage of zinc-based batteries is that zinc is cheap, abundant, and green. Higher energy density in terms of both weight (Wh kg^{-1}) and volume (Wh L^{-1}) is also expected when compared with conventional batteries such as nickel–metal hydride, since the nominal voltage of the zinc–nickel oxide battery (1.6 V) is higher than the nickel–metal hydride battery (1.2 V).

The primary issue limiting use of zinc anodes in rechargeable batteries is the short cycle life caused by dendrite formation upon charging [1]. This non-uniform electrodeposition occurs since the system is strongly non-linear and far from equilibrium, and is controlled by Poisson-type formulations [2]. One method to bring the system closer to equilibrium is to change the mass transport of zincate from diffusion control to convection control by making use of flowing electrolyte [3–9].

The effects of flowing electrolyte on zinc morphology on charging have been investigated over a few decades [3–9]. Experiments have been carried out by a number of researchers under various conditions, and various morphologies of zinc electrodeposits have been identified, including flat, mossy (bulbous), and dendritic. These studies have also shown that the charge rate and the electrolyte velocity strongly affect the morphology. However, these parameters have often been set at values unrealistic for practical battery applications. In addition, the obtained results are not always consistent among the studies. Further, many works have focused on zinc morphology at sub-micron to micron scales, which implies very early stages of electrodeposition. However, zinc morphology at micron to millimeter scales can also significantly influence battery performance.

Among zinc-based rechargeable batteries, the zinc–nickel oxide battery has several advantages including the use of readily available materials, relatively low levels of toxicity, and a fairly high level of safety. Most zinc–nickel oxide batteries have been designed in a sealed and electrolyte-starved configuration, with non-flowing electrolyte [9–11]. Flow-assisted zinc–nickel oxide batteries have been reported by several workers. Bronoel et al. [12] tested a 100 Ah battery. They concluded that a periodic inversion of the electrolyte flow direction allows dissolution of the dendrites formed during the previous sequence, though the system and experimental conditions were complex. Cheng et al. [13] and Zhang et al. [14] have recently clarified basic characteristics of the flow-assisted zinc–nickel oxide battery by cyclic voltammetry experiments. They achieved 220 charge–discharge cycles while keeping the Coulombic and energy efficiencies about 98% and 88%, respectively. They also found that

* Corresponding author at: Department of Chemical Engineering, City College of New York, 140th St at Convent Ave., Steinman Hall #314, New York, NY 10031, USA. Tel.: +1 212 650 8136; fax: +1 212 650 6660.
E-mail address: yito@che.ccny.cuny.edu (Y. Ito).

0378-7753/$ – see front matter © 2010 Elsevier B.V. All rights reserved.
doi:10.1016/j.jpowsour.2010.09.065

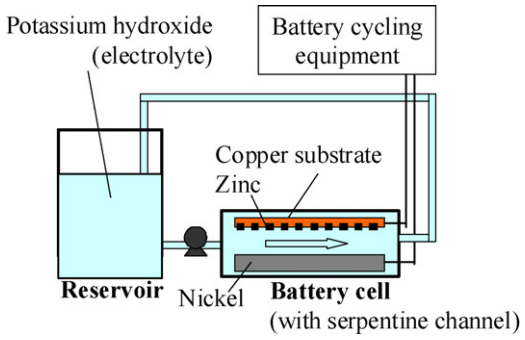

Fig. 1. Experimental apparatus.

cadmium is the best material of several tested as a substrate for zinc deposition, apparently since hydrogen evolution is suppressed most effectively. In their experiments, the flow velocity was fixed to 19.5 cm s^{-1} and the spacer thickness between electrodes was 5 mm. Wills et al. [8] also used similar parameters in their experiments with flow-assisted lead–acid batteries.

Considering the energy density of zinc–nickel oxide flow-assisted batteries, slower electrolyte velocity leads to better performance, since the pressure drop and energy consumption by a pump can be minimized. The spacer thickness between electrodes also affects energy density. The flow gap of 5 mm used by other workers is relatively large, considering typical nickel oxide – separator – zinc electrode cell sandwich thickness are of the order of 2–4 mm.

The purpose of this study centered on experimentally investigating the morphology of zinc on repeated charging and discharging of zinc–nickel oxide flow-assisted batteries. This was done from a relatively macroscopic viewpoint with examining deep discharge cycling. Scale-up of the system was also carried out.

2. Experimental

Fig. 1 shows the schematic of the experimental apparatus. Sintered nickel oxide plates (Jiangsu Highstar Battery Manufacturing) were used as the positive electrodes (cathodes). Zinc as negative electrodes (anodes) was deposited on polished copper foils used as substrates. The electrochemical reaction and standard potential vs. SHE are:

Positive:

$$2NiOOH + 2H_2O + 2e- = 2Ni(OH)_2 + 2OH-, \quad E_0 = 0.49\,V,$$

Negative:

$$Zn + 2OH- = Zn(OH)_2 + 2e-, \quad E_0 = -1.24\,V,$$

Overall:

$$Zn + 2H_2O + 2NiOOH = 2Ni(OH)_2 + Zn(OH)_2, \quad E_0 = 1.73\,V.$$

The capacity of the battery cell tested was 3.7 Ah. The channel had the dimensions of 13 mm in width and 1000 mm in length, and the spacer thickness between two electrodes was 3.1 mm. The positive and negative electrodes were embedded to the channel walls. Zinc oxide (Fisher Scientific ACS Grade) was pre-mixed into 45 wt% potassium hydroxide solution (Fisher Scientific) as electrolyte at a concentration of 50 g L^{-1}. The electrolyte was circulated through the battery cell and the reservoir by a pump. Note that a separator was not needed in the cell. The flow velocity of the electrolyte and the Reynolds number based on the velocity and the hydraulic diameter of the channel were set to 1.6–25.7 cm s^{-1} and 77–1234, respectively. Galvanostatic battery cycling tests were carried out for the charge rates of $C/4$–$1.5C$ (10–60 mA cm^{-2}). Charging was terminated when a battery cell was charged to the full capacity based on the nickel electrode capacity, and discharging was terminated when the voltage dropped to 1.2 V.

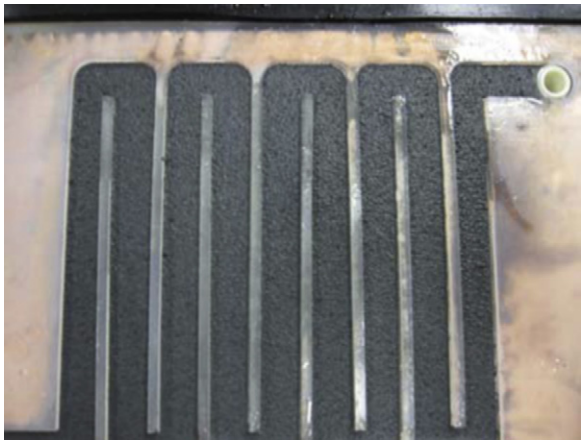

Fig. 2. Electrodeposition of zinc.

3. Results and discussion

Fig. 2 shows an image of the zinc deposited after charging. From this image, it is confirmed that the zinc morphology was the same throughout the active area. In order to reduce the volumetric flow rate of electrolyte while keeping velocity constant, a smaller cross-sectional area and longer flow path are desired. This image suggests that if a battery cell is scaled up in capacity by increasing the length of flow in the streamwise direction, uniform zinc morphology is to be expected.

Fig. 3 shows a battery performance map under different combinations of electrolyte velocities and charge rates. A circle means the battery ran over 200 cycles with discharge capacity >80% of nominal, and Coulombic efficiency more than 85%. A cross means that it did not meet these criteria. The Coulombic efficiency versus cycle number is shown for good- and bad-performing cases in Fig. 4. It is found from Fig. 3 that the flow velocity has little impact on performance when the charge rate is low. However, the performance deteriorated in the cases of higher charge rates and low velocities. High flow velocities (>15 cm s^{-1}) were needed for good performance when the charge rate was high. Fig. 5 shows the charge–discharge curve for (a) good- and (b) bad-performing cases, respectively. For the good cases, the voltage goes up on charging and it gets steeper at the end of charge, since the capacity of positive electrode was maximized and oxygen is generated. When discharging, the cell voltage drops drastically after reaching 1.5 V.

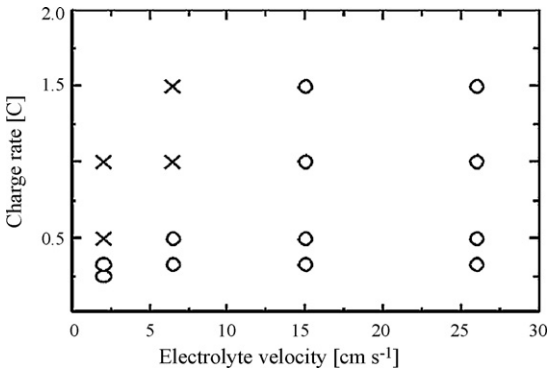

Fig. 3. Battery performance map (circle: good performance; cross: bad performance).

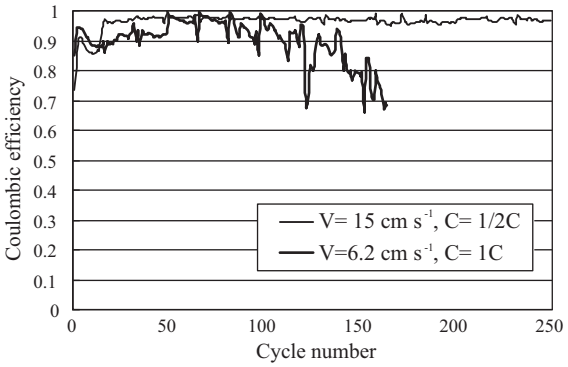

Fig. 4. Coulombic efficiency vs. cycle number.

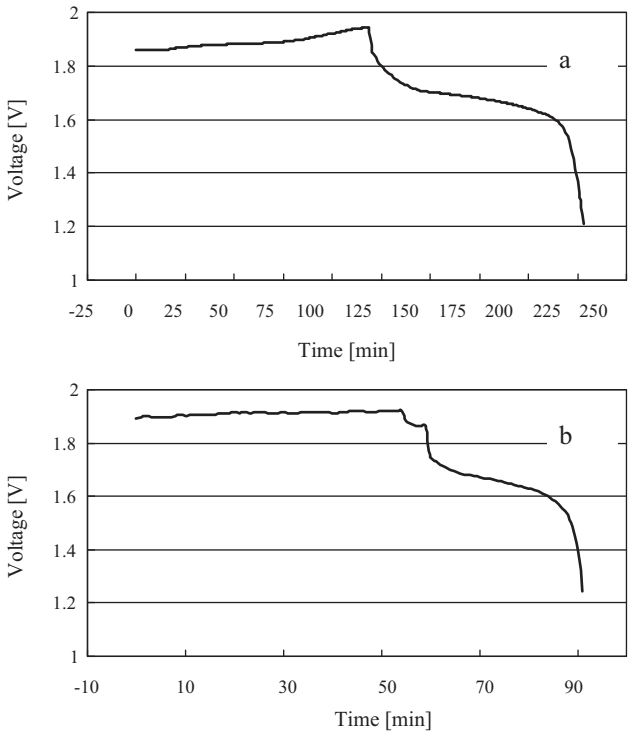

Fig. 5. Charge–discharge curve: (a) $V = 15\,\mathrm{cm\,s^{-1}}$ and $C = 1/2C$; (b) $V = 6.2\,\mathrm{cm\,s^{-1}}$ and $C = 1C$.

For the poorly performing cases, the curve on charging does not go up and levels off or even drops with fluctuations. We believe that this is caused by internal short circuits which have developed in the cell.

For better understanding this behavior, time lapsed images of the internal flow path inside a single straight cell were captured by a stereo microscope (Amscope ZM-4TW3-FOR-5 M). The channel configuration of this cell was the same as the cell mentioned above except the length was 150 mm and the walls were made of transparent acrylic. The images were captured at the center of the channel. Fig. 6 shows the images taken at (a) 1st, (b) 5th, and (c) 9th cycles from fresh surface at a charge rate of $C/3$ and a flow velocity of $1.6\,\mathrm{cm\,s^{-1}}$. The zinc morphology is mossy but relatively uniform during early cycles. However, the zinc deposited on charge does not fully dissolve into electrolyte on discharging; areas of spotty deposition remain on the substrate. This is due to the higher Coulombic efficiency of the zinc electrode versus the nickel oxide electrode. This residual zinc becomes the nuclei of electrodeposition during the subsequent cycles. Zinc electrodeposition is enhanced at these locations, since the current density at these points is higher than at the others. The net effect is that the zinc deposit progressively approaches the cathode on extended cycling. In addition, these images indicate that when the spacer thickness between electrodes is too small, zinc growths more readily contact the positive electrode, leading to deteriorated electrical performance.

To compare the effect of charge rate, the test was repeated, but at a $1C$ charge rate. The result is shown in Fig. 7. The growth of the zinc deposit toward the cathode in the $1C$ case occurs more rapidly than that of the $C/3$ case. Contact of the zinc deposit with the nickel electrode also occurs sooner. The zinc morphology is still mossy but the non-uniformity becomes more pronounced on subsequent cycles. Since the porosity is quite high and the zinc is not in strong

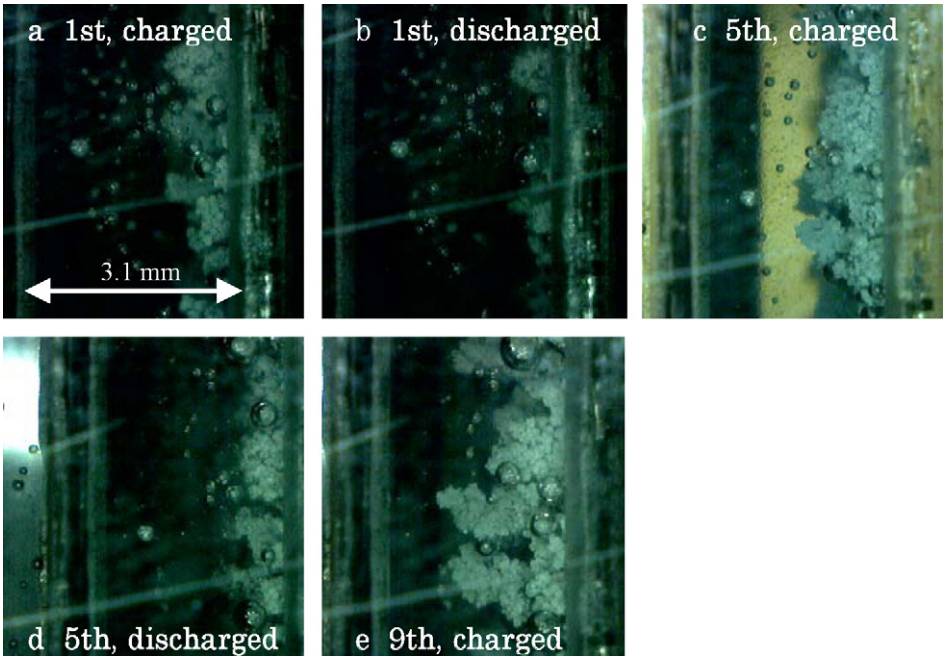

Fig. 6. Electrodeposition of zinc ($V = 2\,\mathrm{cm\,s^{-1}}$, $C = 1/3C$): (a) 1st cycle, charged; (b) 1st cycle, discharged; (c) 5th cycle, charged; (d) 5th cycle, discharged; (e) 9th cycle, charged.

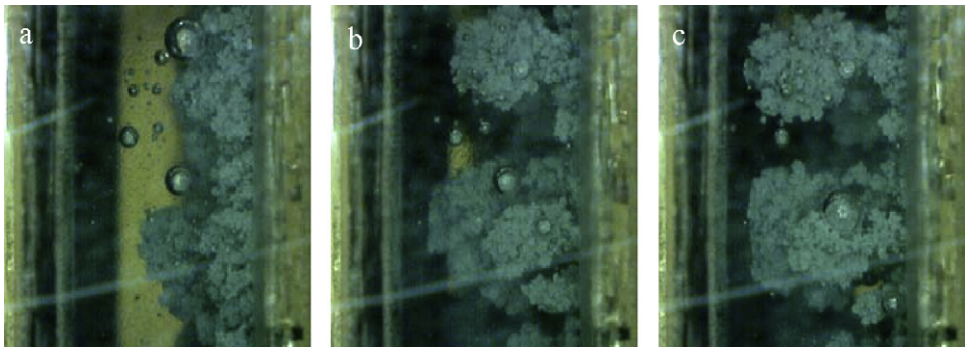

Fig. 7. Electrodeposition of zinc ($V = 2\,\mathrm{cm\,s^{-1}}$, $C = 1C$): (a) 1st cycle; (b) 5th cycle; (c) 9th cycle.

contact with the nickel electrode (e.g. soft short circuit), performance was not greatly affected. However, this difference may help explain why the performance was poor at higher charge rates.

In both cases, the zinc deposit was flat at the very beginning of charge. Non-uniformity was observed soon thereafter, and the dendritic electrodeposition of zinc was not suppressed by the flow. However, if we calculate the theoretically required electrolyte velocity to avoid non-uniformity of electrodeposition of zinc due to lack of zincate ion, it is far less than our experimental conditions, since an excess amount of zinc is initially supplied. In fact, even the flow velocity of $1\,\mathrm{mm\,s^{-1}}$ is enough to change the system from diffusion control to convection control. Therefore, limitation of mass transfer for zinc ion at macro scale may not be the reason of this non-uniform electrodeposition. It is possibly caused by the non-uniformity of the substrate, whereas the mass transfer of metal ion was changed from diffusion control to convection control which is close to equilibrium. In fact, as found in the experiments by Sutija et al. [4], a substrate with 5 μ projections strongly affects the zinc morphology.

In this sense, the faster electrolyte velocity is not expected to modify the morphology of zinc. However, as shown in the battery performance map (Fig. 4), the performance was stable for higher velocity cases. Fig. 8, the images after charging at a charge rate of 1*C* and a flow velocity of $15\,\mathrm{cm\,s^{-1}}$, provide the reason. It is clearly seen that the direction of dendrite growth of zinc is distorted and bent toward the flow direction, probably due to shear stress based on flowing electrolyte, in particular when zinc comes close to the positive side. Therefore, although the dendritic growth of zinc itself is not suppressed by the flowing electrolyte, internal short circuiting is much less likely to happen and the deterioration of performance was prevented. In addition, oxygen evolved from Ni electrode may contribute to zinc dissolution for the faster velocity cases, since mixing is enhanced and there is a greater opportunity to direct oxygen bubbles toward the negative electrodes.

As mentioned above, the zinc deposited on charging does not dissolve into the solution completely on discharging, leading to internal short circuits fairly quickly—within several tens of cycles. In order to reduce the capacity fade, the batteries were subjected to a reconditioning procedure every 15 charge–discharge cycles. The reconditioning procedure consisted of a very slow discharge at a *C*/15 rate to the voltage of 0.6 V. As shown in Fig. 9, which is the case at $1.6\,\mathrm{cm\,s^{-1}}$ velocity and 1*C* charge rate, the zinc is gradually stripped from the substrate until it is altogether removed. After the reconditioning cycle, the surface is renewed and the electrodeposition of zinc becomes relatively flat and uniform again. From a practical point of view, the spacer thickness between the electrodes may be determined by an acceptable frequency of reconditioning for a given application.

The charge/discharge capacity and the Coulombic and energy efficiencies versus cycle number are shown in Figs. 10 and 11, respectively, for a flow velocity of $15\,\mathrm{cm\,s^{-1}}$ and a *C*/2 charge rate. The cell has been running for 1500 cycles, and is still running as of this writing. Coulombic and energy efficiencies of over 90% and 80%, respectively, have been maintained. The efficiencies are not as high as those reported by Zhang et al. [14] and Cheng et al. [13], probably because the positive electrode capacity was maximized in our experiments. However, our cell still performed far better than conventional Zn–NiOOH cells using non-flowing electrolyte, which typically obtain only a few hundred cycles. The instability of performance is probably caused by gas generated due to electrolysis occurring as side reaction. When bubbles are not removed near the negative plates, they act as an obstacle and promote the dendritic growth of zinc in the vicinity of the bubble, as shown in Fig. 12.

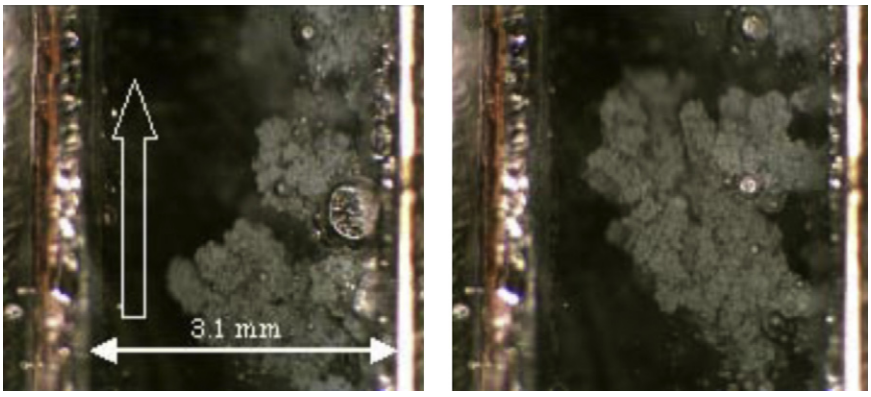

Fig. 8. Electrodeposition of zinc ($V = 15\,\mathrm{cm\,s^{-1}}$, $C = 1C$): (a) 1st cycle; (b) 9th cycle.

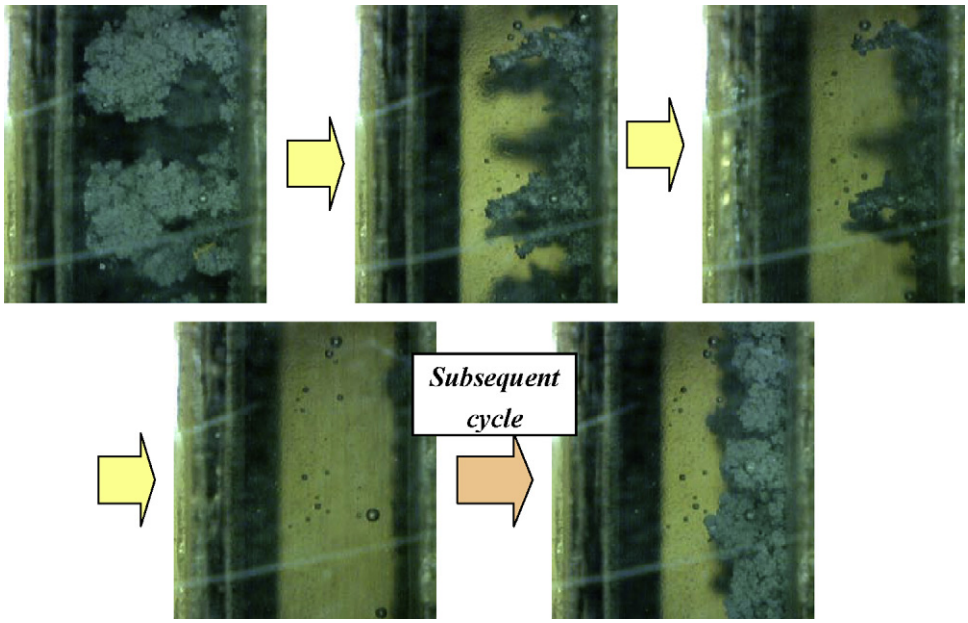

Fig. 9. Zinc dissolution at a reconditioning cycle.

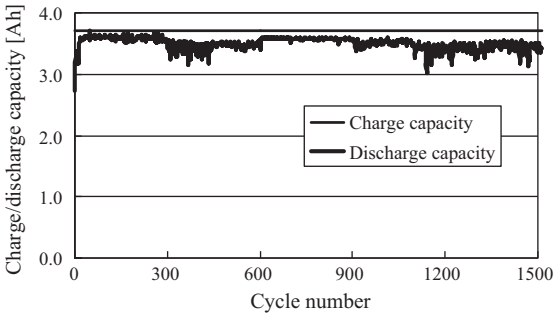

Fig. 10. Charge/discharge capacity vs. cycle number for the 3.7 Ah battery.

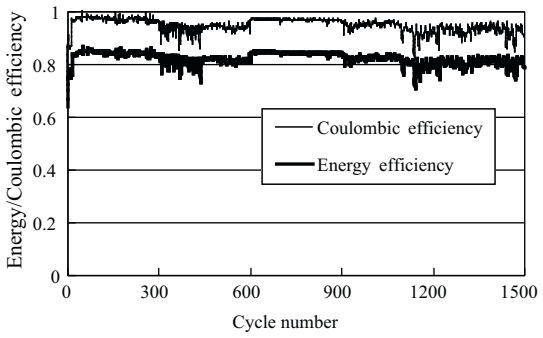

Fig. 11. Coulombic and energy efficiencies vs. cycle number for the 3.7 Ah battery.

4. Scale up

Fig. 13 is a picture of a 100 Wh (1.6 V–60 Ah) prismatic cell developed based on these earlier experiments. Alternately layered via spacers (thickness = 2.4 mm) were 12 positive and 13 negative electrodes. Washers as spacers (diameter = 3.1 mm) were placed every 30 mm in both the streamwise and spanwise directions. The electrolyte consisted of 45% KOH solution, into which 120 g L^{-1} ZnO was dissolved. The electrolyte flows from the bottom to the top of the cell at an average velocity of 5 mm s^{-1}. Cycling is being conducted at *C*/7 charge and discharge rates. These cycling rates were determined by a consideration of several potential utility applications. As shown in Figs. 14 and 15, the battery has been running in a stable fashion; the Coulombic and energy efficiencies are almost the same as those for the 3.7 Ah cell after 200 cycles. Though further testing is needed for better understanding and optimization for large scale applications such as traction and stationary energy storage, it was shown that Zn–NiOOH flow-assisted battery is potentially suitable for large-scale energy storage systems.

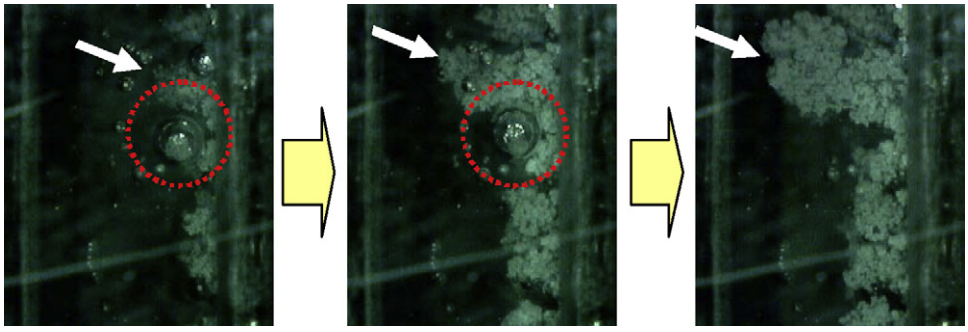

Fig. 12. Effect of a bubble on electrodeposition of zinc.

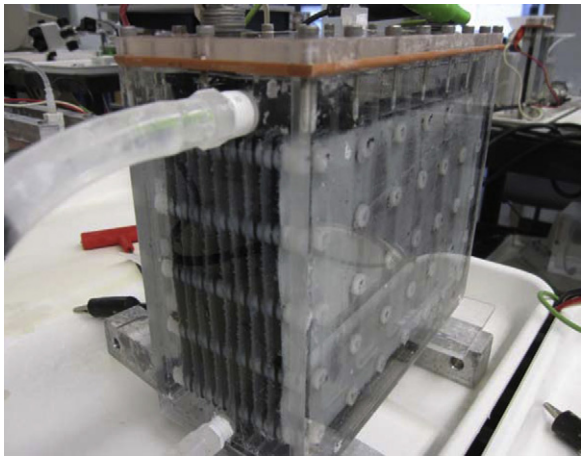

Fig. 13. The 100 Wh Zn–Ni flow battery.

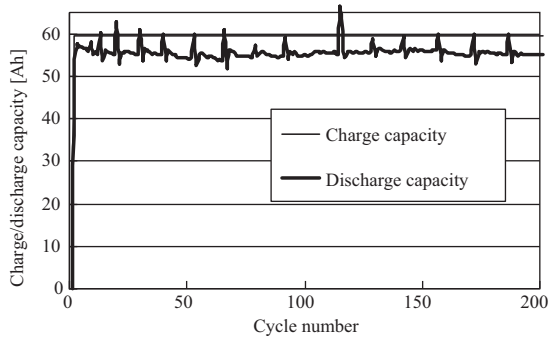

Fig. 14. Charge/discharge capacity vs. cycle number for the 100 Wh battery.

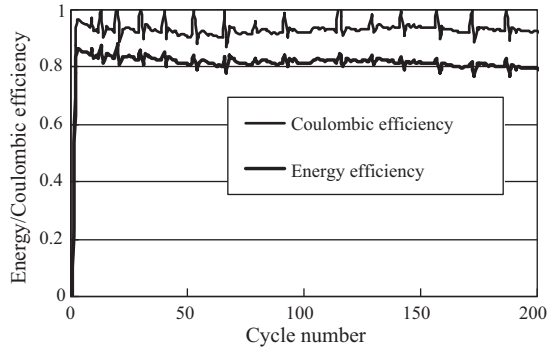

Fig. 15. Charge/discharge capacity vs. cycle number for the 100 Wh battery.

5. Conclusions

An experimental study of the morphology of zinc obtained by repeatedly charging and discharging flow-assisted zinc–nickel oxide cells was carried out. In general, one can associate the morphology with the electrical performance of the cells. The main conclusions are as follows:

- Flowing electrolyte contributes to better performance for the Zn–NiOOH cells.
- Higher charge rates lead to more dendritic zinc deposits on charging and tend to result in degraded cell performance. When the electrolyte velocity is higher than 15 cm s^{-1}, the direction of dendrites was distorted toward the flow direction and internal short circuit was suppressed.
- 1500 stable cycles were achieved by using periodic reconditioning procedures, which demonstrated the long-life potential of the flow-assisted Zn–NiOOH system.
- A Zn–NiOOH flow-assisted battery is potentially suitable for energy storage systems at large scales.

Acknowledgements

This work was performed under a grant from the New York State Foundation for Science (NYSTAR). The authors express great appreciation to Dr. Joshua Gallaway (City College of New York), Prof. Alvin Salkind, and Mr Allen Charkey for their useful discussions.

References

[1] D. Linden, T.B. Reddy (Eds.), Handbook of Batteries, third ed., 2001.
[2] K. Fukami, S. Nakanishi, H. Yamasaki, T. Tada, K. Sonoda, N. Kamikawa, N. Tsuji, H. Sakaguchi, Y. Nakato, J. Phys. Chem. C 111 (2007) 1150.
[3] R.D. Naybour, J. Electrochem. Soc. 116 (1969) 520.
[4] D.P. Sutija, R.H. Muller, C.W. Tobias, J. Electrochem. Soc. 141 (1994) 1477.
[5] J. Jorne, M.G. Lee, J. Electrochem. Soc. 143 (1996) 865.
[6] R.Y. Wang, D.W. Kirk, G.X. Zhang, J. Electrochem. Soc. 153 (2006) C357.
[7] F.R. McLarnon, E.J. Cairns, J. Electrochem. Soc. 138 (2) (1991) 1.
[8] R.G.A. Wills, J. Collins, D. Stratton-Campbell, T.J. Low, D. Pletcher, F.C. Walsh, J. Appl. Electrochem. 40 (2010) 955.
[9] Z.P. Arkhangel'skaya, M.M. Loginova, T.B. Kas'yan, D.A. Vinogradova, Rus. J. Appl. Chem. 77 (2004) 67.
[10] Z.P. Arkhangel'skaya, A.I. Demidov, M.M. Loginova, T.B. Kas'yan, E.V. Apollonova, Rus. J. Appl. Chem. 78 (2005) 1430.
[11] P.H.L. Notten, E. Verbitskiy, W.S. Kruijt, H.J. Bergvelda, J. Electrochem. Soc. 152 (2005) A1423.
[12] G. Bronoel, A. Millot, N. Tassin, J. Power Sources 34 (1991) 243.
[13] J. Cheng, L. Zhang, Y.S. Yang, Electrochem. Commun. 9 (2007) 2639.
[14] L. Zhang, J. Cheng, Y.S. Yang, J. Power Sources 179 (2008) 381.